A Numerical Analysis of Electric Field Strength Over Planar Microarray Dot Electrode for Dielectrophoretic Lab-On-Chip Device

B. Yafouz[1], N.A. Kadri[1], F. Ibrahim[1]

[1] Medical Informatics and Biological Micro-Electro-Mechanical Systems (MIMEMS) Specialized Laboratory, Department of Biomedical Engineering, Faculy of Engineering, University of Malaya, 50603 Kuala Lumpur, Malaysia

***Abstract*—Dielectrophoresis (DEP) has been proven as a method of manipulating and analyzing the electrophysiological properties of bioparticles by applying non-uniform electric fields generated through special electrodes. Various electrode geometries have been developed to address different applications. Simulation of the electric field strength over electrodes is essential in order to optimize the generated DEP force for enhancing cell manipulation. This paper describes the study of electric field distribution over planar multiple microarray dot electrode using numerical modeling of Comsol Multiphysics 4.2a®. Results show that the electric field strength is axisymmetrical around the centre of the dot aperture and that is higher at the dot edges than the dot centers. Further studies will be conducted to investigate the effect of applying different frequencies, varying dots size and adding ground plane in between the electrode dots.**

***Keywords*—Lab-on-Chip, dielectrophoresis, numerical modeling, dot microarray electrodes**

I. INTRODUCTION

Microfluidic devices have the potential to be used for early detection and diagnosis of disease at Point-of-Care (POC). This is aligned with the current trend of miniaturizing laboratory equipment to achieve better reactions efficiency, faster results, portability and lower reagents consumption. One of the platforms used in microfluidic devices is Lab-on-chip, which is a potential solution for an automated bio-microfluidic diagnostic system that requires the minimum quantity of blood and offers fast and high-throughput results.

Many diagnostic techniques have been employed using lab-on-chip platforms; however, dielectrophoresis (DEP) has been proven to offer a number of advantageous features that many of the other techniques available are unable to provide. These include high selectivity and efficacy, non-invasiveness and low cost. DEP has been used as a method for cell manipulation and characterization since its discoverer Pohl [1] launched a novel technique for separating living cells from admixed dead ones, taking advantage of the unique electrical properties of each bioparticle [2].

DEP is the phenomenon that describes the motion of polarizable particles through a non-uniform electric field. One of the core strengths of DEP is that the characterization of different cells depends only on the dielectric properties controlled by the particle's individual phenotype. Hence, the process does not require specific tags or involve chemical reactions [3].

The DEP force depends on the applied frequency and geometry of the electrodes used to generate the electric field. Different electrode geometries have been used in previous studies for different applications. This study provides a numerical analysis of the electric field generated by a 4x4 planar multiple microarray dot electrode, which is a modification of that used by Fatoyinbo *et al.* [4]. This electrode will be used to conduct DEP expirements as a sample preparation prior to the stage of infectious dieases diagnosis.

A. Dielectrophoretic Theory

Applying a non-uniform electric field to polarizable particles that are placed in a conductive medium produces DEP force. The magnitude and direction of the DEP force depend on the relative polarizability of the particle and the surrounding medium [5]. The DEP force acting on a spherical particle can by expressed by the following equation [6]:

$$\langle \vec{F}_{DEP} \rangle = 2\pi r^3 \varepsilon_o \varepsilon_m \, \mathrm{Re}[K(\omega)] \nabla E^2 \tag{1}$$

where ε_o is the permittivity of free space, ε_m is the permittivity of the surrounding medium, r is the particle radius, ∇E is the electric field gradient and $Re[K(\omega)]$ is the real part of Clausius-Mossotti factor which is defined as:

$$K(\omega) = \frac{\varepsilon_p^* - \varepsilon_m^*}{\varepsilon_p^* + 2\varepsilon_m^*} \tag{2}$$

where ε^* is the complex permittivity and subscripts p and m denote particles and medium, respectively. Moreover, the complex permittivity ε^* is described by:

$$\varepsilon^* = \varepsilon - j\frac{\sigma}{\omega} \tag{3}$$

where ε is the permittivity, $j = \sqrt{-1}$, σ is the conductivity and ω is the angular frequency of the applied AC electric field. The value of $Re[K(\omega)]$ for a sphere ranges between -0.5 and 1, and depends on the frequency of the applied AC

electric field and relative polarizability between the particle and its surrounding medium [6]. When $Re[K(\omega)] > 0$, the particles undergo positive DEP and move toward the high electric field gradient region. However, when $Re[K(\omega)] < 0$, the particles travel to the low electric field gradient region as a result of the negative DEP effect.

B. Electrode Design

In order to minimize the value of the applied voltage, the non-uniform electric field required for DEP is typically produced by electrodes on the scale of microns. Electrode geometries can be categorized into two main groups: planar and 3D electrodes.

Planar electrodes are typically patterned on the bottom of the microchannel using conventional lithography techniques. Examples of planar electrode designs include interdigitated [7], castellated [8], spiral [9], curved [10], oblique [11], quadrupole [12], matrix [4] and polynomial [13].

On the other hand, 3D electrodes are designed on the bottom, bottom/top, or side wall of the microchannel using complicated techniques. Examples of 3D electrode designs are grid [14], microwells [15], DEP-well [16], extruded [17], sidewall patterned [18] and top-bottom patterned [19]. This variety of electrode geometry has evolved in response to the need to address different research tasks. Hence, the electrode geometry is determined by the general goal of the study.

A planar multiple microarray dot electrode was chosen in this study because it has a well-defined and enclosed region of analysis. Furthermore, this type of electrode has been proven to create electric fields with axisymmetrical gradient around every dot aperture [20]. Moreover, the current 4x4 dot array electrode was designed such that individual dots can be electrically supplied independently, giving the capability to observe and record cellular electrophysiological changes in near real-time by conducting multiple DEP experiments in parallel.

II. METHODOLOGY

AC/DC module of Comsol Multiphysics 4.2a® (COMSOL Inc, Palo Alto, USA) was used to model the electric field distribution over the microarray dot electrode. A few assumptions were made to mimic the actual situation and to provide greater processing memory and a better fitting mesh of the model.

As shown in Fig. 1, the designed 3D model represents a gasket chamber sandwiched between a bottom patterned electrode and a top "ground" electrode. Fig. 1a illustrates the total electrode size of 22 x 22 mm^2. The top ground electrode was modeled as a 5x5x0.1 mm^3 solid block, while the gasket chamber was represented by 3x3x1 mm^3 solid block, as depicted in Fig. 1b. Fig. 1c demonstrates the bottom patterned electrode with dot diameter, dots separation and ring width of 200, 150 and 50 µm, respectively. The patterned electrode was given a thickness of 0.1 mm.

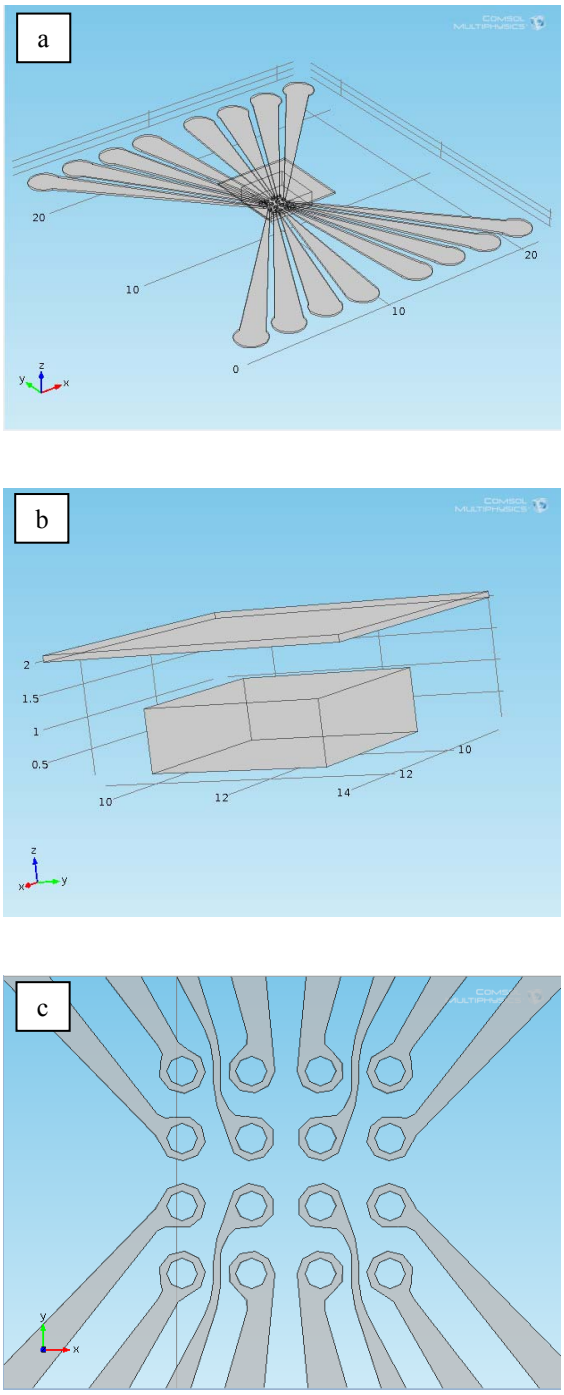

Figure 1. Three dimensional model of the planar multiple microarray dot electrode showing (a) the full design, (b) ground electrode and the gasket chamber, and (c) the 4x4 dot microarray electrode.

The patterned dot electrode was given gold properties $\sigma = 4.1x10^7$ S/m and $\varepsilon_r = 1$, the ground electrode was given material properties of indium tin oxide (ITO) $\sigma = 1.3x10^4$ S/m and $\varepsilon_r = 10$. Finally, the gasket chamber, which represents the suspending medium, was given the material properties of deionized water $\sigma = 2x10^{-4}$ S/m and $\varepsilon_r = 78$ [20, 21].

Meshing was done for the entire geometry using a tetrahedral element type with the maximum and minimum element sizes as 5 and 0.05mm, respectively (Fig. 2). Boundary condition for the top electrode was defined as ground, while the patterned electrode was supplied with $10V_p$, and the frequency was set to 100 kHz.

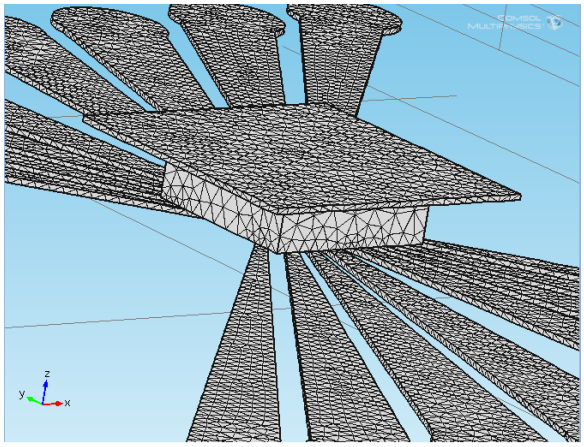

Figure 2. The designed electrode structure after meshing using tetrahedral elements.

III. RESULTS AND DISCUSSION

After building the model, assigning materials properties, meshing and setting the boundary conditions, the model was simulated and the electric field strength (V/m) was plotted as shown in Fig. 3. The results revealed that the values of the electric field strength at the edge of the dots are higher than that at the center of the dots for all electrode designs. Therefore, the DEP force is expected to be higher at the dot edges rather than at the dot centers, which is in agreement with the findings of Fatoyinbo *et al.* [20]

Also, Fig. 3 illustrates that the electric field strengths are axisymmetrical around the centre of the aperture of the dots, which suggests that the DEP force is also axisymmetrical within the dot volume. This indicates that the particles will undergo homogenous radial movement. The direction of this movement will depend on Clausius-Mossotti factor. If it is positive, particles will be attracted to the dot edges. However, if Clausius-Mossotti factor is negative, particles will be repelled to the centers of the dots.

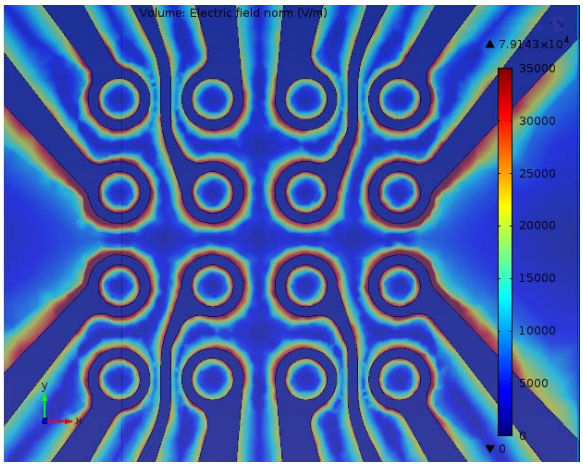

Figure 3. Electric field strength (V/m) distribution over 200µm dot array electrode.

IV. CONCLUSION

A numerical analysis of the electric field distribution over multiple microarray dot electrode has been demonstrated. Results have shown that the electric field strength is axisymmetrical around the centre of the dot aperture, and that is higher at the edges of the dots than at center of the dots. Further studies will be conducted to investigate the effect of applying different frequencies on each dot and observe the change in DEP force as a result of the dependency of Clausius-Mossotti factor on the applied signal frequency. The electric field strengths will also be compared for different dot sizes. Finally, the effect of adding ground plane between the apertures of the dots will be evaluated.

ACKNOWLEDGMENT

This research is financially supported by the University of Malaya, Ministry of Higher Education High Impact Research Grant (UM/HIR/MOHE/ENG/05), and the University of Malaya Research Grant (UMRG: RG023/09AET).

REFERENCES

[1] H. A. Pohl, "The motion and precipitation of suspensoids in divergent electric fields," *Journal of Applied Physics,* vol. 22, pp. 869-871, 1951.

[2] H. A. Pohl and I. Hawk, "Separation of living and dead cells by dielectrophoresis," *Science,* vol. 152, p. 647, 1966.

[3] N. A. Kadri, "Development of near real-time assessment system for cancer cells," Doctor of Philosophy PhD Thesis, Centre for Biomedical Engineering University of Surrey 2011.

[4] H. O. Fatoyinbo, N. A. Kadri, D. H. Gould, K. F. Hoettges, and F. H. Labeed, "Real time cell electrophysiology using a multi channel dielectrophoretic dot microelectrode array," *Electrophoresis,* vol. 32, pp. 2541-2549, 2011.

[5] R. Pethig and G. H. Markx, "Applications of dielectrophoresis in biotechnology," *Trends in biotechnology,* vol. 15, pp. 426-432, 1997.

[6] J. Cao, P. Cheng, and F. Hong, "A numerical analysis of forces imposed on particles in conventional dielectrophoresis in

microchannels with interdigitated electrodes," *Journal of Electrostatics,* vol. 66, pp. 620-626, 2008.

[7] J. Auerswald and H. F. Knapp, "Quantitative assessment of dielectrophoresis as a micro fluidic retention and separation technique for beads and human blood erythrocytes," *Microelectronic engineering,* vol. 67, pp. 879-886, 2003.

[8] F. F. Becker, X. B. Wang, Y. Huang, R. Pethig, J. Vykoukal, and P. Gascoyne, "Separation of human breast cancer cells from blood by differential dielectric affinity," *Proceedings of the National Academy of Sciences,* vol. 92, p. 860, 1995.

[9] X. B. Wang, Y. Huang, X. Wang, F. F. Becker, and P. Gascoyne, "Dielectrophoretic manipulation of cells with spiral electrodes," *Biophysical journal,* vol. 72, pp. 1887-1899, 1997.

[10] K. Khoshmanesh, C. Zhang, F. J. Tovar-Lopez, S. Nahavandi, S. Baratchi, K. Kalantar-zadeh, and A. Mitchell, "Dielectrophoretic manipulation and separation of microparticles using curved microelectrodes," *Electrophoresis,* vol. 30, pp. 3707-3717, 2009.

[11] M. S. Pommer, Y. Zhang, N. Keerthi, D. Chen, J. A. Thomson, C. D. Meinhart, and H. T. Soh, "Dielectrophoretic separation of platelets from diluted whole blood in microfluidic channels," *Electrophoresis,* vol. 29, pp. 1213-1218, 2008.

[12] L. S. Jang, P. H. Huang, and K. C. Lan, "Single-cell trapping utilizing negative dielectrophoretic quadrupole and microwell electrodes," *Biosensors and Bioelectronics,* vol. 24, pp. 3637-3644, 2009.

[13] M. P. Hughes and H. Morgan, "Dielectrophoretic trapping of single sub-micrometre scale bioparticles," *Journal of Physics D: Applied Physics,* vol. 31, p. 2205, 1998.

[14] J. Suehiro and R. Pethig, "The dielectrophoretic movement and positioning of a biological cell using a three-dimensional grid electrode system," *Journal of Physics D: Applied Physics,* vol. 31, p. 3298, 1998.

[15] R. S. Thomas, H. Morgan, and N. G. Green, "Negative DEP traps for single cell immobilisation," *Lab Chip,* vol. 9, pp. 1534-1540, 2009.

[16] K. F. Hoettges, Y. Hübner, L. M. Broche, S. L. Ogin, G. E. N. Kass, and M. P. Hughes, "Dielectrophoresis-activated multiwell plate for label-free high-throughput drug assessment," *Analytical chemistry,* vol. 80, pp. 2063-2068, 2008.

[17] C. Iliescu, L. Yu, F. E. H. Tay, and B. Chen, "Bidirectional field-flow particle separation method in a dielectrophoretic chip with 3D electrodes," *Sensors and Actuators B: Chemical,* vol. 129, pp. 491-496, 2008.

[18] L. Wang, J. Lu, S. A. Marchenko, E. S. Monuki, L. A. Flanagan, and A. P. Lee, "Dual frequency dielectrophoresis with interdigitated sidewall electrodes for microfluidic flow-through separation of beads and cells," *Electrophoresis,* vol. 30, pp. 782-791, 2009.

[19] M. Dürr, J. Kentsch, T. Müller, T. Schnelle, and M. Stelzle, "Microdevices for manipulation and accumulation of micro-and nanoparticles by dielectrophoresis," *Electrophoresis,* vol. 24, pp. 722-731, 2003.

[20] H. O. Fatoyinbo, K. F. Hoettges, and M. P. Hughes, "Rapid-on-chip determination of dielectric properties of biological cells using imaging techniques in a dielectrophoresis dot microsystem," *Electrophoresis,* vol. 29, pp. 3-10, 2008.

[21] Serway and Raymond, *Principles of Physics*, 2nd ed. Fort Worth, Texas; London: Saunders College Publishing, 1998.